Korean J. Chem. Eng., 35(11), 2220-2231 (2018)
DOI: 10.1007/s11814-018-0146-1

pISSN: 0256-1115
eISSN: 1975-7220

An organofunctionalized $MgO \cdot SiO_2$ hybrid support and its performance in the immobilization of lipase from *Candida rugosa*

Agnieszka Kołodziejczak-Radzimska†, Jakub Zdarta, Filip Ciesielczyk, and Teofil Jesionowski

Institute of Chemical Technology and Engineering, Faculty of Chemical Technology,
Poznan University of Technology, Berdychowo 4, PL-60965, Poznan, Poland
(*Received 7 May 2018 • accepted 28 August 2018*)

Abstract−Lipase from *Candida rugosa* was immobilized on $MgO \cdot SiO_2$ hybrid grafted with amine, thiol, cyano, phenyl, epoxy and carbonyl groups. The products were analyzed using Fourier transform infrared spectroscopy, nuclear magnetic resonance, low-temperature N_2 sorption and elemental analysis. Additionally, the degree of coverage of the oxide material surface with different functional groups and the number of surface functional groups were estimated. The Bradford method was used to determine the quantity of immobilized enzyme. The largest quantity of enzyme (25-28 mg/g) was immobilized on the hybrid functionalized with amine and carbonyl groups. On the basis of hydrolysis reaction of *p*-nitrophenyl palmitate to *p*-nitrophenol, it was determined how the catalytic activity of the obtained biocatalysts is affected by pH, temperature, storage time, and repeated reaction cycles. The best results for catalytic activity were obtained for the lipase immobilized on $MgO \cdot SiO_2$ hybrids with amine and carbonyl groups. The biocatalytic system demonstrated activity above 40% in the pH range 4-10 and in the temperature range 30-70 °C. Lipase immobilized on the $MgO \cdot SiO_2$ systems with amine and epoxy groups retains, respectively, around 80% and 60% of its initial activity after 30 days of storage, and approximately 60-70% after 10 reaction cycles.

Keywords: Hybrid Oxide Materials, Surface Grafting, Lipase from *Candida rugosa*, Enzyme Immobilization, Enzymatic Activity and Stability

INTRODUCTION

The choice of an appropriate support is of key importance for the overall feasibility of industrial applications of immobilized enzymes. The support should have the capacity to immobilize as large as possible a quantity of the protein on its surface. The hydrophobicity of the surface should usually be minimized, since it favors undesired protein adsorption and denaturation. The support must also contain functional groups that enable the functionalization and activation of the matrix. These groups should provide high surface density while minimizing steric hindrance. After immobilization, however, the support should be completely inert under the working conditions of the enzyme, not interfering with the desired reaction. A suitable support should also offer chemical resistance, thermal stability, mechanical strength, insolubility in the reaction environment, and high surface area. The support should be relatively inexpensive and not harmful to the environment, minimizing the economic impact of the process [1-9]. Substances with the aforementioned properties include mesoporous silica-based materials [10], having pore diameters in the range 2-50 nm and surface areas in the range 300-1,500 m^2 [1].

In carrying out the immobilization process, attention must be paid to the correct preparation of the matrix. Supports are not usually capable of connecting directly to proteins; hence they are activated using substances that ensure the reactivity of the matrix with functional groups of the enzyme being immobilized. Activation of a support involves the introduction onto its surface of appropriate groups (including -OH, -NH, -C=O, -SH, -COC) which are responsible for electrophilic functions. In this way a functionalized matrix is obtained, and the introduced chemical groups improve the effectiveness of the immobilization process and cause the enzyme to be more durably attached.

Mesoporous silicates (MPS) are attractive materials for use as supports in the immobilization of enzymes [11-14]. MPS synthesis is relatively straightforward and produces materials with well-defined and ordered porous structures, high surface areas and good mechanical and chemical stability. Functionalization of the surface of an MPS can be tailored to favor the immobilization of a particular enzyme [15-17]. The porous structure of an MPS can provide a very stable environment for enzymes, with substantial increases in stability versus that observed for the enzyme in solution. This stability can be obtained without significant loss in catalytic activity [18].

The attractiveness of these compounds is confirmed by literature reports concerning the immobilization of various enzymes on their surface. There have been studies [19,20] in which catalase and glucose oxidase were immobilized on the surface of Florisil (a commercial magnesium silicate). Lipase, in turn, has been immobilized primarily on mesoporous materials such as SBA, PPS and MPS [21-23]. Hybrids materials are characterized with well-developed porosity. Combined and reinforced materials usually exhibit properties not observed for their individual components. Moreover, hybrid supports in general provide a suitable environment for bio-

†To whom correspondence should be addressed.
E-mail: agnieszka.kolodziejczak-radzimska@put.poznan.pl

molecules that favors the retention of high catalytic properties by the immobilized enzyme, makes the biocatalytic system reusable and protects it against conformational changes during storage [9, 24,25]. Up to now, hybrid materials used in the enzyme immobilization process are, for example, hybrids containing Fe_3O_4 [26-32], polyaniline-polyacrylonitrile composite, polyacrylonitrile-multi-walled carbon nanotubes [25,33] and others [34-36].

In general, inorganic hybrids exhibit good chemical and thermal stability, mechanical resistance and chemical inertness. Moreover, their precursors are easily available and in many cases their synthesis is simple and hence relatively cheap. The hydroxyl groups (-OH) present on their surface determine the hydrophilic character of these materials. Additionally, the presence of many functional groups increases affinity of the hybrid supports to biomolecules, enhances immobilization efficiency and allows easy functionalization of the surface [37,38]. Besides simple modification, the presence of various chemical moieties allows the production of combined materials with desired technological features and high affinity for enzymes, which makes these materials promising for practical applications [9,39,40]. Based on this information, in the present work for the first time, organofunctionalized-MgO·SiO_2 was used as a support for the immobilization of lipase from *Candida rugosa*. The magnesium silicate surface was functionalized using glutaraldehyde and silane coupling agents containing amine, thiol, phenyl, cyano and glycidoxy groups. The porous structure of the resulting systems was then analyzed. A key stage in the study was the determination of the effect of the type of functional groups on the quantity of immobilized enzyme and on the properties of the resulting systems. The effectiveness of the immobilization process was determined by the Bradford method and by analysis of FTIR and NMR spectra. The effect of pH and temperature on catalytic activity, as well as the systems' storage stability and reusability, were investigated based on a model reaction in which *p*-nitrophenyl palmitate was hydrolyzed to *p*-nitrophenol.

MATERIALS AND METHODS

1. Materials

In the synthesis of magnesium silicate, an aqueous solution of sodium metasilicate (general formula $Na_2O{\cdot}mSiO_2{\cdot}xH_2O$, produced by Vitro-Silicon S.A.) and a solution of magnesium sulfate (VI) (obtained from pure $MgSO_4{\cdot}7H_2O$, produced by Chempur) were used. The modifiers used for surface functionalization of MgO·SiO_2 were 3-aminopropyltriethoxysilane (APTES), 3-mercaptopropyltrimethoxysilane (MPTMS), phenyltriethoxysilane (PTES), 3-cyanopropyltriethoxysilane (CPTES), 3-glycidyloxypropyltrimethoxysilane (GPTMS) and glutaraldehyde (GA), purchased from Sigma Aldrich. Lipase from *Candida rugosa* (LCR), monobasic sodium phosphate (NaH_2PO_4), dibasic sodium phosphate (Na_2HPO_4) *p*-nitrophenyl palmitate (*p*-NPP), *p*-nitrophenol (*p*-NP), 2-propanol, Triton X-100 and Arabic gum were purchased from Sigma Aldrich (Saint Louis, MO, USA).

Table 1 lists the properties of the modifiers used and the names of the samples obtained.

2. Synthesis and Surface Grafting of MgO·SiO_2

MgO·SiO_2 was synthesized by the classical precipitation method

Table 1. Characterization of used modifiers and description of obtained samples

Modifier	Groups	Structural formula	Sample acronym
3-Aminopropyltriethoxysilane (A)	-NH	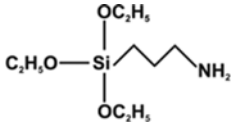	MgO·SiO_2_A
3-Mercaptopropyltrimethoxysilane (M)	-SH	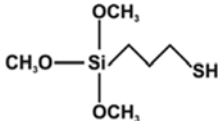	MgO·SiO_2_M
3-Cyanopropyltriethoxysilane (C)	-CN	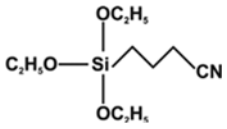	MgO·SiO_2_C
Phenyltriethoxysilane (P)	-C_6H_5	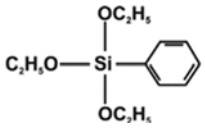	MgO·SiO_2_P
3-Glicydoxypropyltrimethoxysilane (G)	-COC	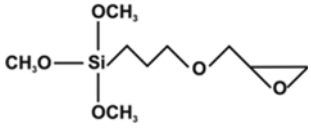	MgO·SiO_2_G
Glutaraldehyde (GA)	-C=O	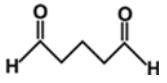	MgO·SiO_2_GA

developed by Ciesielczyk et al. [41]. To a reactor containing a 5% solution of magnesium sulfate, an appropriate quantity of sodium silicate was added. The system was stirred, and the reaction was allowed to proceed until the pH of the suspension reached a value of 5-6. The mixture was then filtered under pressure, and the resulting precipitate was dried and sieved. Dry $MgO{\cdot}SiO_2$ powder was modified using silane modifying compounds (APTES, MPTMS, TEPS, CPTES, GPTES) and glutaraldehyde (GA). Modification was performed using a "dry method" [42,43]: the silane coupling agents were firstly hydrolyzed in a methanol/water system (4 : 1, v/v) and then sprayed directly onto the surface of the synthetic magnesium silicate. The silane coupling agents were used in an amount of 3 wt/wt [44,45]. Modification with glutaraldehyde was performed by pouring a 5% solution of glutaraldehyde over an appropriate quantity of $MgO{\cdot}SiO_2$. The system was stirred for 24 h at room temperature, and was then filtered under pressure and dried. Fig. 1 shows a schematic representation of the process of synthesis and modification of magnesium silicate. The codes used for the obtained samples are given in Table 1.

3. Immobilization of Lipase from *Candida rugosa* on Grafted $MgO{\cdot}SiO_2$ Hybrid

The immobilization process was carried out by a covalent method. A defined quantity of the previously prepared support was immersed in a solution of lipase from *Candida rugosa* (3 mg/mL, 0.2 M solution of phosphate buffer (PBS) at pH=7). The process was continued for 24 h at room temperature, after which the immobilized system was filtered and dried, again at room temperature. All protein concentrations were determined by the Bradford method [46], using bovine serum albumin (BSA) as standard. The quantity (P) of lipase from *Candida rugosa* deposited on the modified $MgO{\cdot}SiO_2$ was calculated from Eq. (1):

$$P = \frac{(C_0 - C_1)\cdot V}{m} \quad (1)$$

where C_0 and C_1 denote the concentration of the enzyme (mg/mL) in solution before and after immobilization, respectively, V is the volume of solution (mL), and m is the mass of modified $MgO{\cdot}SiO_2$ (g).

Fig. 2 shows a schematic representation of the immobilization process.

4. Physicochemical Analysis of Samples

To identify the characteristic groups present on the surface of the products, samples were subjected to FTIR analysis using a Vertex 70 spectrophotometer (Bruker, Germany). The samples were analyzed in the form of KBr tablets, as KBr crystals are inactive in the IR range. The analysis was performed over a wavenumber range of 4,000-400 cm^{-1}.

^{13}C CP MAS NMR analysis of the prepared materials was performed in a DSX spectrometer (Bruker, Germany). A sample of about 100 mg was placed in a ZrO_2 rotator 4 mm in diameter, which enabled spinning of the sample. Centrifugation at the magic angle was performed at a spinning frequency of 8.4 kHz. The ^{13}C CP MAS

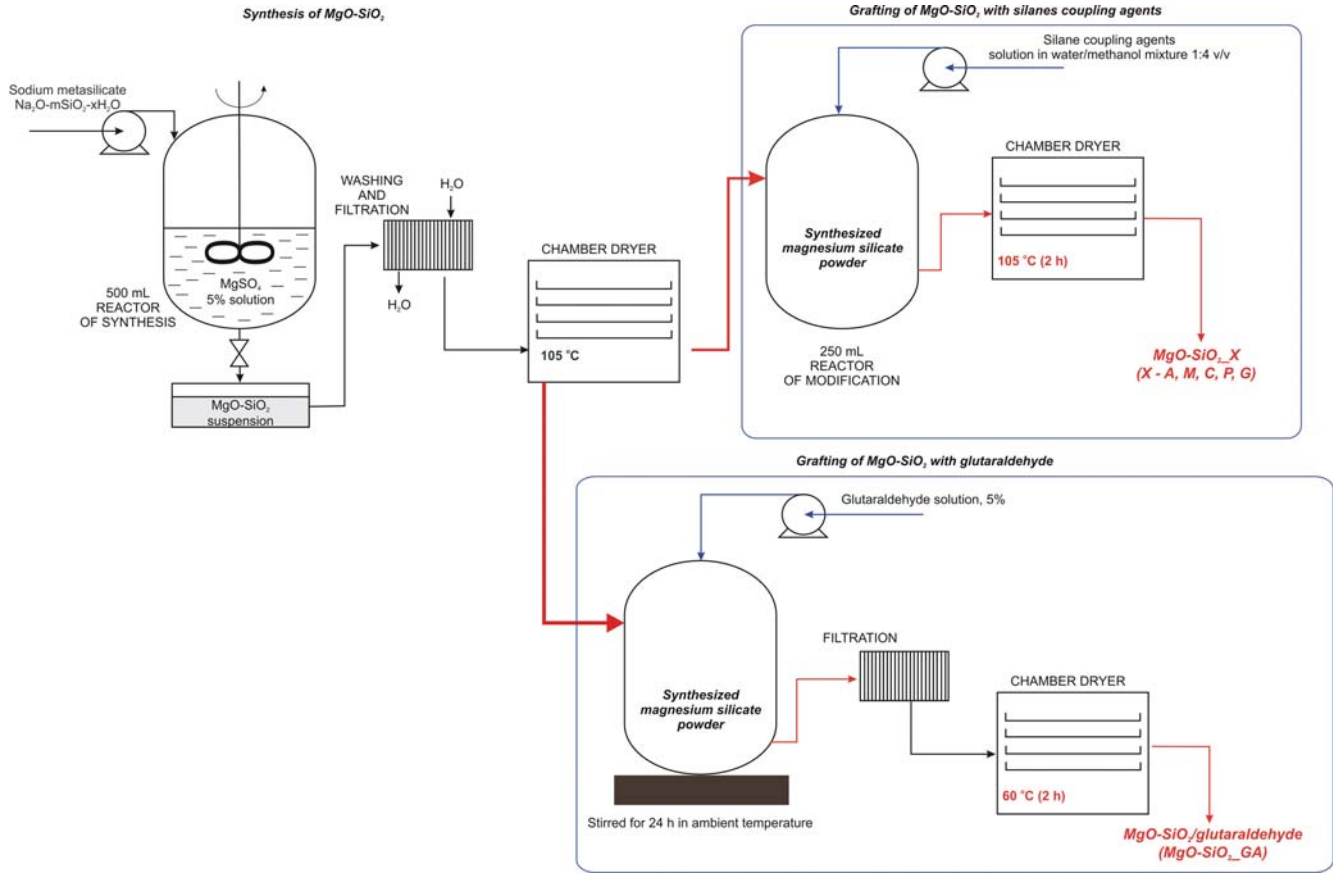

Fig. 1. Schematic diagram of synthesis and modification of $MgO{\cdot}SiO_2$ hybrid.

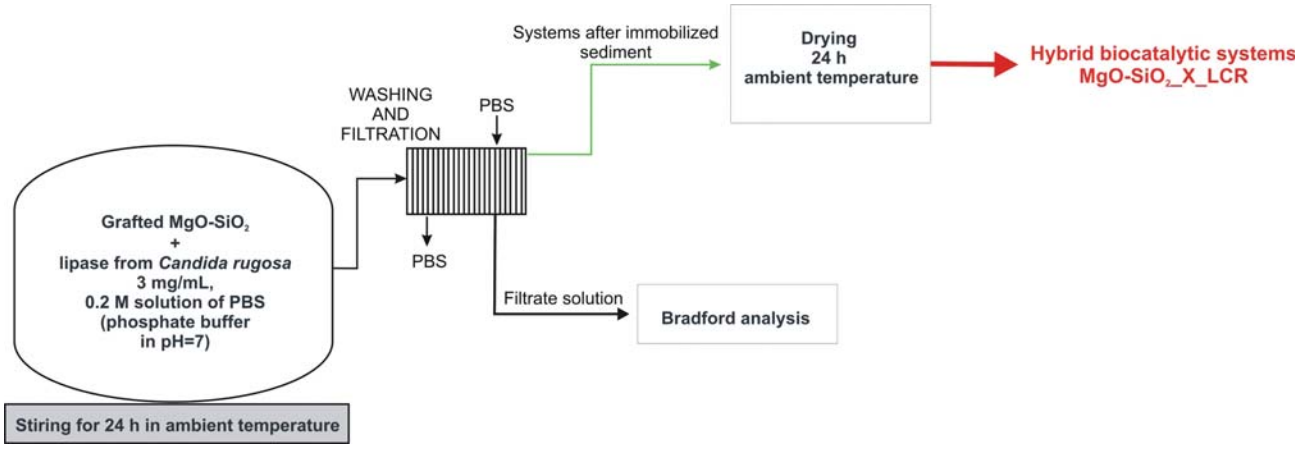

Fig. 2. Schematic diagram of the immobilization of lipase onto grafted MgO·SiO_2 hybrid.

NMR spectra were recorded at 100.63 MHz in a standard 4 mm MAS probe by application of single pulse excitation with high-power proton decoupling (pulse repetition 10 s, spinning speed 10 kHz).

Low-temperature N_2 sorption was also applied. The surface area (A_{BET}), total pore volume (V_p) and mean pore diameter (S_p) were determined using an ASAP 2020 instrument (Micromeritics Instrument Co., USA). All samples were degassed at 120 °C for 4 h prior to measurement. The surface area was determined by the multipoint BET (Brunauer-Emmett-Teller) method using the adsorption data as a function of relative pressure (p/p_0). The BJH (Barrett-Joyner-Halenda) algorithm was applied to determine the total pore volume and the mean pore diameter. Due to the high accuracy of the instrument used, surface area was determined to an accuracy of ±0.1 m^2/g, pore volume to ±0.01 cm^3/g, and pore size to ±0.01 nm.

The elemental composition of the materials was established with a Vario El Cube instrument (Elementar Analysensysteme GmbH, Germany), which gave the percentage content of carbon, nitrogen and hydrogen after high-temperature combustion of the analyzed samples. Results are given as averages for three measurements, each accurate to ±0.0001%. The degrees of coverage of the MgO·SiO_2 support with the modifiers were also evaluated from the results of elemental analysis, using the Berendsen and de Golan equation [27]:

$$P = \frac{10^6 \cdot C}{[1200 \cdot N_c - C(M-1)] \cdot A} \quad (2)$$

where P (μmol/m^2) is the degree of coverage, C is the percentage content of carbon from elemental analysis, N_c is the number of carbon atoms in the attached molecule, M is the molar mass of the attached compound, and A is the surface area of the support.

Further, the number of surface functional groups N_R (nm^{-2}), which reflects the density of modifier grafted on the MgO·SiO_2 surface, was calculated from the results of elemental analysis and BET measurement. N_R is defined as the number of aminopropyl, mercaptopropyl, phenyl, cyanopropyl, glycidyloxypropyl and carbonyl groups on the MgO·SiO_2 surface per nm^2, and is calculated from the following equation [47]:

$$N_R = \frac{C \cdot N_A}{12 \cdot n \cdot 100 \cdot S} \quad (3)$$

where C is the percentage content of carbon from elemental analysis, n is the number of carbon atoms in a molecule of the silane coupling agent excluding methoxy groups, N_A is Avogadro's number, and S is the surface area of the sample.

5. Enzyme Assay

The hydrolytic activity of the immobilized enzymes was estimated according to the methodology described by Zdarta et al. [48]. Briefly, the spectrophotometric measurements were based on the ability of the enzymes to transform *p*-NPP (*p*-nitrophenyl palmitate) into *p*-NP (*p*-nitrophenol). The release of the product was observed at 410 nm (using a JASCO V650 spectrophotometer, Japan). All reactions (performed in triplicate) were carried out with stirring at 100 rpm for 2 min at 30 °C.

6. Evaluation of Stability of Free Lipase and Immobilization Products

The effect of temperature on the activity of free and immobilized aminoacylase was examined from 30-80 °C, at pH=7. The effect of pH was tested over a range of 4-10, at 30 °C. All determinations were based on the hydrolysis of *p*-NPP to *p*-NP.

The reusability of the immobilized lipase was studied by measuring the residual enzyme activities repeatedly on 12 cycles. After each reaction, the enzyme was separated from the substrate solution by centrifugation and washed with fresh phosphate buffer (pH=7). The retention of activity was determined under optimal conditions (30 °C, 2 min and pH=7).

We also investigated how the enzymatic activity of the immobilized systems is affected by conditions of storage. For this purpose the systems were immersed in a buffer solution at pH=7 and stored for 30 days at room temperature or at approximately 4 °C. Every five days samples were filtered and dried, and their enzymatic activity was tested by the procedure described above.

All measurements were made in triplicate. Results are presented as mean ±3.0 SD.

RESULTS AND DISCUSSION

1. FTIR and NMR Analysis

Unmodified and modified MgO·SiO_2 underwent comprehensive physicochemical analysis to determine the effectiveness of the

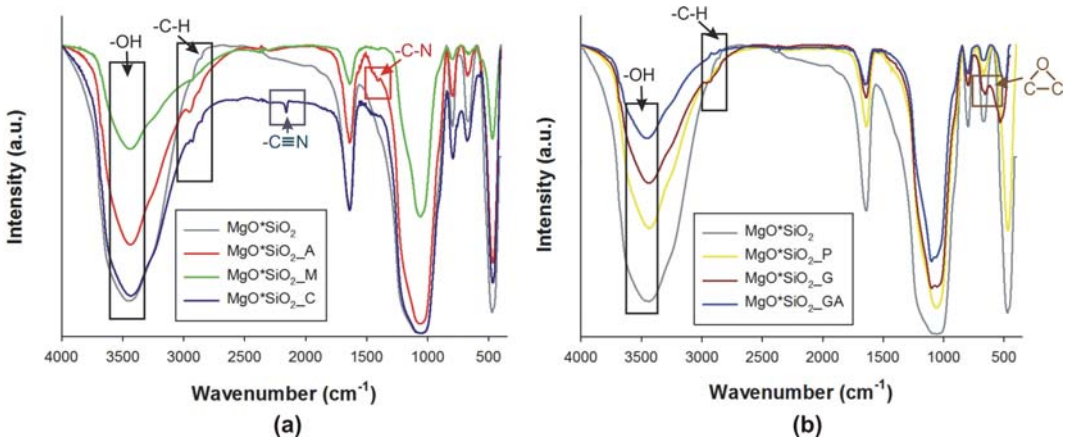

Fig. 3. FTIR spectra of unmodified $MgO{\cdot}SiO_2$ and oxide materials modified with amine, thiol and cyano groups (a); phenyl, epoxy and carbonyl groups (b).

modification process. FTIR spectra of the products are shown in Fig. 3.

As previously stated, one of the main goals of this study was to confirm the possibility of using an inorganic $MgO{\cdot}SiO_2$ hybrid material as an effective support for enzymes. The FTIR spectrum of the inorganic mixed oxide matrix (Fig. 3(a)) shows a broad signal in the wavenumber range 3,600-3,400 cm^{-1}, characteristic for stretching vibrations of hydroxyl groups. This shows that the material was susceptible to surface modification and effective enzyme attachment. The spectrum also contains signals at 1,100, 800 and 650 cm^{-1}, generated by stretching vibrations of Si-O-Si, Si-O and Si-O-Mg bonds, respectively, which confirm the composition of the material [49].

FTIR spectra were then examined to confirm the effective functionalization of the hybrid material with amine, thiol and cyano groups (Fig. 3(a)) and with phenyl, epoxy and carbonyl groups (Fig. 3(b)). All of the spectra revealed a significant decrease in the intensity of the characteristic signal for -OH groups. There also appeared bands related to stretching vibrations of -C-H bonds, characteristic for the aliphatic chains of the modifiers, in the wavenumber range 2,900-2,800 cm^{-1}, indicating that the modifying agents were successfully attached to the surface of the support [50]. In addition, signals attributed to functional moieties present in the structure of the functionalizer, such as a peak at 2,240 cm^{-1} (stretching vibrations of C≡N in the spectrum of $MgO{\cdot}SiO_2$_C), a signal with a maximum around 1,400 cm^{-1} (stretching vibrations of C-N bonds in the spectrum of $MgO{\cdot}SiO_2$_A) or bands at around 800 and 530 cm^{-1} (stretching vibrations of C-O-C bonds and deformational vibrations of epoxy rings in the spectrum of $MgO{\cdot}SiO_2$_G) proved the presence of these groups in the analyzed samples, and hence confirmed the successful surface functionalization.

To provide indirect confirmation of the effectiveness of the immobilization process, FTIR spectra were obtained for the systems following immobilization (Fig. 4).

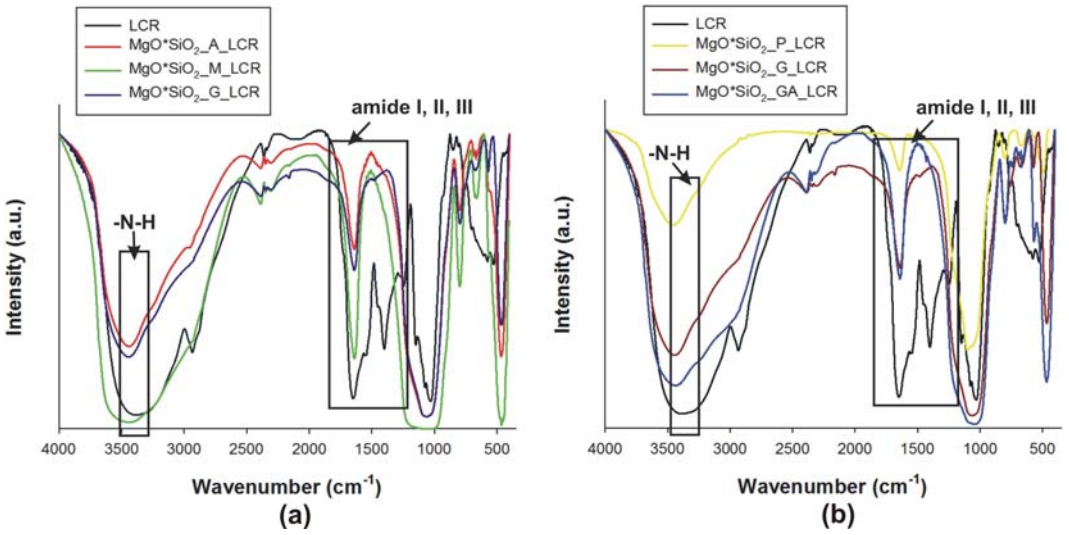

Fig. 4. FTIR spectra of free lipase and of the enzyme immobilized on an $MgO{\cdot}SiO_2$ system modified with amine, thiol and cyano groups (a); phenyl, epoxy and carbonyl groups (b).

Fig. 4 shows the FTIR spectrum of free lipase from *Candida rugosa* and the spectra of the produced biocatalytic systems with immobilized enzyme. The spectrum of free LCR contains four major signals, characteristic for the protein backbone of the enzyme: a band centered at 3,420 cm^{-1}, attributed to stretching vibrations of N-H bonds in -NH_2 groups (which are mainly responsible for attachment of the enzyme); an amide I band with maximum at 1,653 cm^{-1}, originating from stretching vibrations of carbonyl groups; an amide II band at 1,543 cm^{-1}; and an amide III absorption band at wavenumber 1,415 cm^{-1}, derived from bending vibrations of N-H bonds and stretching vibrations of C-N bonds [51]. In the spectra of the immobilized enzyme, irrespective of the modifying agent used, there are changes in the intensity of the signals in the wavenumber ranges 3,600-3,300 cm^{-1} and 2,950-2,800 cm^{-1} compared with the spectra of the support before immobilization. Moreover, in the wavenumber range characteristic for amide bands, the spectra of the systems after immobilization contain peaks of low intensity, indicating the presence of the biocatalysts in the analyzed samples [52]. It can be concluded that the changes in intensity and broadening of the bands characteristic for the relevant functional groups indirectly confirm the effective deposition of the lipase onto the surface of the inorganic oxide system.

Changes confirming the success of the modification and immobilization processes were also observed on the carbon nuclear magnetic resonance spectra for systems modified with amine and epoxy groups (Fig. 5). The spectra of MgO·SiO_2_A (Fig. 5(a)) and MgO·

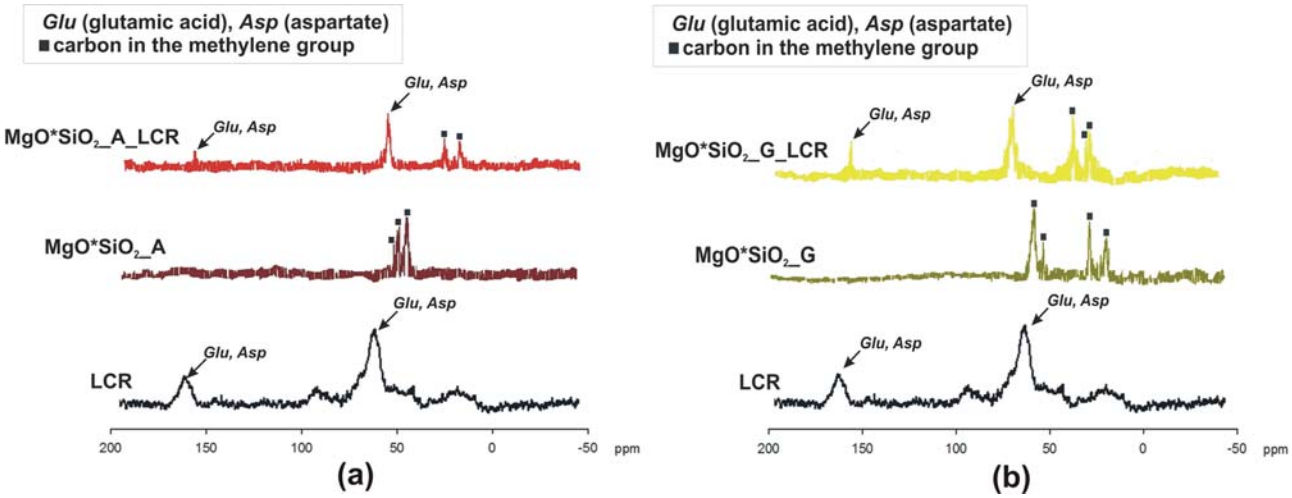

Fig. 5. ^{13}C CP MAS NMR spectra of the supports, free lipase, and lipase immobilized on MgO·SiO_2 with amine groups (a); MgO·SiO_2 with epoxy groups (b).

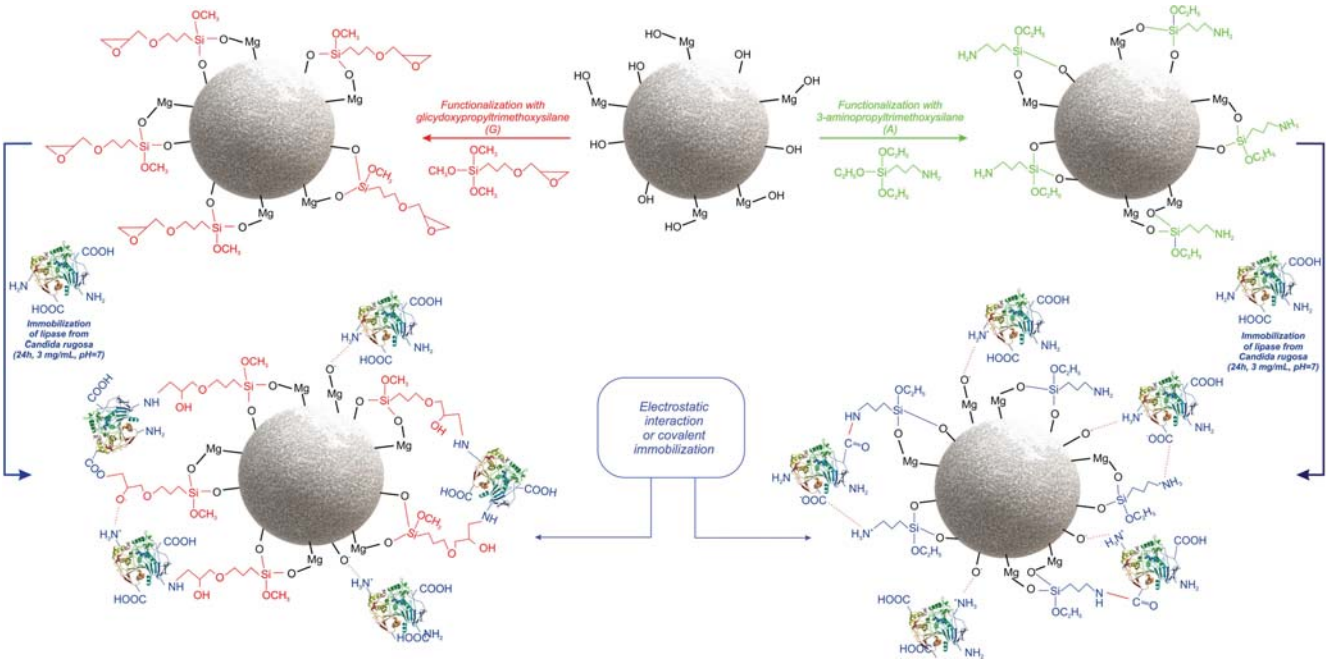

Fig. 6. Probably mechanism of immobilization of lipase onto MgO·SiO_2 modified with amino- and epoxy groups.

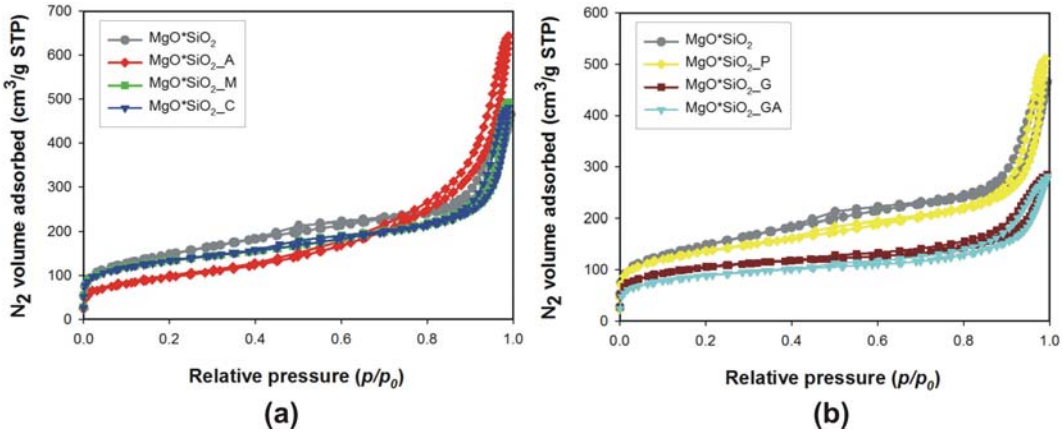

Fig. 7. Nitrogen adsorption/desorption isotherms of unmodified MgO·SiO_2 and the support modified with amine, thiol and cyano groups (a); phenyl, epoxy and carbonyl groups (b).

SiO_2_G (Fig. 5(b)) contain many signals (20-55 ppm) originating from the carbon in the methylene group (-CH_2) in the modifier structures [53]. The spectrum for lipase (Fig. 5) contains two clear signals at chemical shifts of 70 and 170 ppm, attributed to carbon atoms from certain amino acids (*Glu*, glutamic acid and *Asp*, aspartate), as well as several bands of much smaller intensity and wider range [54]. The spectra of the systems following immobilization (MgO·SiO_2_A_LCR, Fig. 5(a); MgO·SiO_2_G_LCR, Fig. 5(b)) display signals originating from both the support and the enzyme. There is a characteristic signal at 170 ppm which was not observed in the spectra of the supports. Analysis of the ^{13}C CP MAS NMR spectra confirms the effectiveness of the immobilization of the enzyme on the modified magnesium silicate.

Fig. 6 presents the probable mechanism of immobilization of lipase onto MgO·SiO_2 modified with amino- and epoxy groups. The mechanism is based mainly on electrostatic interactions (NH_3^+, COO^-, O^-), but the covalent bonds generated between the enzyme (-NH_2 and -COOH) and silane groups (-NH and -COC) are also of great significance, which was confirmed by the analysis of FTIR and NMR spectra. Irrespective of the type of modification, the contribution of these bonds is associated with the amount and type of silane functional groups in oxide hybrid structure [55-57].

2. Porous Structure Parameters of Supports and Resulting Biocatalysts

An analysis was made of the porous structure of the supports used for immobilization. Fig. 7 shows low-temperature nitrogen adsorption/desorption isotherms for unmodified MgO·SiO_2 and all of its modified forms. All isotherms are of type IV according to the IUPAC classification, indicating the presence of mesopores [58]. Surface areas range from 293 to 520 m^2/g, pore volumes from 0.03 to 0.72 cm^3/g and pore sizes from 5.6 to 12.5 nm (Table 2), showing that these materials have well-developed structures. From the data in Table 2 it can be concluded that the modification process was effective. There was a significant decrease in the surface area and pore volumes in the modified systems compared with pure MgO·SiO_2. Magner [2] has found that mesoporous materials cannot be used as supports for enzymes if their pores are smaller than 3 nm, because these are too small to accommodate enzymes. In

Table 2. Porous structure parameters of unmodified and modified MgO·SiO_2 and samples after immobilization

Sample	Specific surface areas (m^2/g)	Total pore volume (cm^3/g)	Average pore size (nm)
MgO·SiO_2	520	0.72	5.6
MgO·SiO_2_A	339	0.92	12.0
MgO·SiO_2_A_LCR	209	0.03	1.9
MgO·SiO_2_M	444	0.06	9.1
MgO·SiO_2_M_LCR	313	0.03	1.9
MgO·SiO_2_C	444	0.05	8.7
MgO·SiO_2_C_LCR	261	0.03	1.9
MgO·SiO_2_P	455	0.05	9.0
MgO·SiO_2_P_LCR	265	0.03	2.0
MgO·SiO_2_G	344	0.30	12.5
MgO·SiO_2_G_LCR	278	0.29	12.5
MgO·SiO_2_GA	294	0.33	12.2
MgO·SiO_2_GA_LCR	243	0.28	12.5

accordance with this finding, the proposed modified MgO·SiO_2 may prove a good support for enzyme immobilization, since it has pore sizes in the range 8.7-12.5 nm.

At the next stage it was determined how the immobilization process affects the chief porous structure parameters (surface area, pore volume and pore size) of the systems. The results (Table 2) provide indirect confirmation of the effectiveness of the immobilization process. This is evidenced by the smaller surface area values compared with the original supports. Also observed was a significant reduction in the pore sizes of the biocatalytic systems formed by immobilization of the enzyme on supports modified with amine groups (MgO·SiO_2_A_LCR), thiol groups (MgO·SiO_2_M_LCR), cyano groups (MgO·SiO_2_C_LCR) and phenyl groups (MgO·SiO_2_P_LCR). This may be because the enzyme molecules are immobilized inside the pores, or because they block the pore spaces. Additionally, entry of the enzyme into the pores of the MgO·SiO_2 support creates a more stable environment for the protein and prevents damage by external shear forces. Similar findings were reported by Forde et al. [12]. On the other hand, the pore volume and pore size of MgO·SiO_2_G and MgO·SiO_2_GA were not altered by LCR immobilization. This indicates that the LCR molecules do not occupy the mesoporous spaces of MgO·SiO_2_G and MgO·SiO_2_GA, but exist on the outer surface of particles [2,59]. In this case, stable bonds may also have been formed between the enzyme and the functional groups of the support.

3. Elemental Analysis

Direct evidence of the effectiveness of the modification process is provided by the results of elemental analysis (Table 3). The modified samples were found to have an increased carbon content, which results from the introduction of molecules of the modifier onto their surface. Also, the samples modified with APTES and CPTES had nitrogen content of 0.638% and 0.214%, respectively, and the MPTES-modified sample had a sulfur content of 0.775%. Based on the results of elemental analysis and the values of surface area (A_{BET}), a determination was made of the degree of coverage (P) of the support surface with the modifier and of the number of surface functional groups (N_R) (Table 3). The highest degrees of coverage (0.78, 0.43 and 1.19 μmol/m^2) were obtained for the hybrid modified with amine, epoxy and carbonyl groups, respectively, while the smallest values were recorded for samples modified with thiol groups (0.30 μmol/m^2), cyano groups (0.22 μmol/m^2) and phenyl groups (0.25 μmol/m^2). A similar pattern is observed in the case of the number of surface functional groups, which was highest for the samples modified with amine and carbonyl groups (0.20 and 0.12 nm^{-2}, respectively), and for the remaining systems lay in the range 0.03-0.06 nm^{-2}.

Table 3. Elemental analysis, degree of surface coverage and number of surface functional groups for modified MgO·SiO_2 systems

Sample	Content (%)				P	N_R
	N	C	H	S	(μmol/m^2)	(nm^{-2})
MgO·SiO_2	-	0.082	3.071	-	-	-
MgO·SiO_2_A	0.638	4.037	2.487	-	0.78	0.20
MgO·SiO_2_M	-	1.087	1.885	0.775	0.30	0.04
MgO·SiO_2_C	0.214	1.329	1.766	-	0.22	0.04
MgO·SiO_2_P	-	1.815	1.812	-	0.25	0.03
MgO·SiO_2_G	-	2.274	1.696	-	0.43	0.06
MgO·SiO_2_GA	-	3.620	1.866	-	1.19	0.12

4. Characterization of Hybrid Biocatalysts

Fig. 8(a) shows the relative activity of lipase immobilized on modified MgO·SiO_2. The relative activity was highest for lipase immobilized on MgO·SiO_2 modified with amine and carbonyl groups (100% and 76%, respectively). This may be related to the fact that these are the systems on which the greatest quantities of enzyme were immobilized (28.5 mg/g for MgO·SiO_2_A and 25 mg/g for MgO·SiO_2_GA). The same systems (MgO·SiO_2_A and MgO·SiO_2_GA) were also found to have the largest number of surface functional groups (N_R) (Fig. 8(b)). Somewhat smaller values were obtained for the systems MgO·SiO_2_M (39%) and MgO·SiO_2_G (38%), which were also found to have smaller quantities of immobilized enzyme (10 and 14 mg/g, respectively). The smallest values of both relative activity and quantity of immobilized lipase

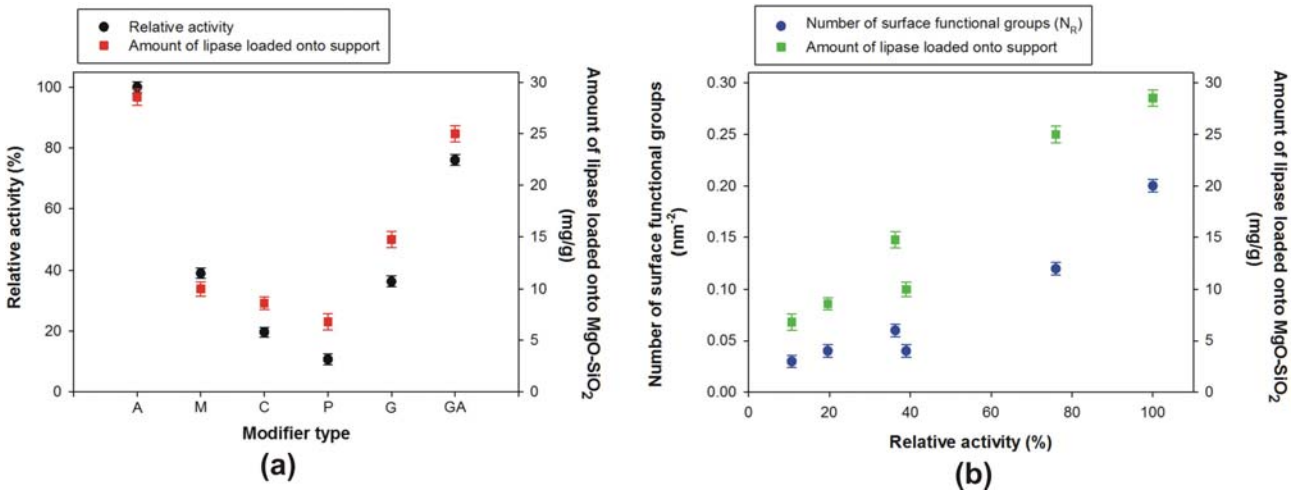

Fig. 8. Relative activity of lipase immobilized on MgO·SiO_2 modified with different groups and quantity of lipase immobilized (a); influence of number of surface functional groups and amount of lipase loaded onto MgO·SiO_2 on relative activity (b).

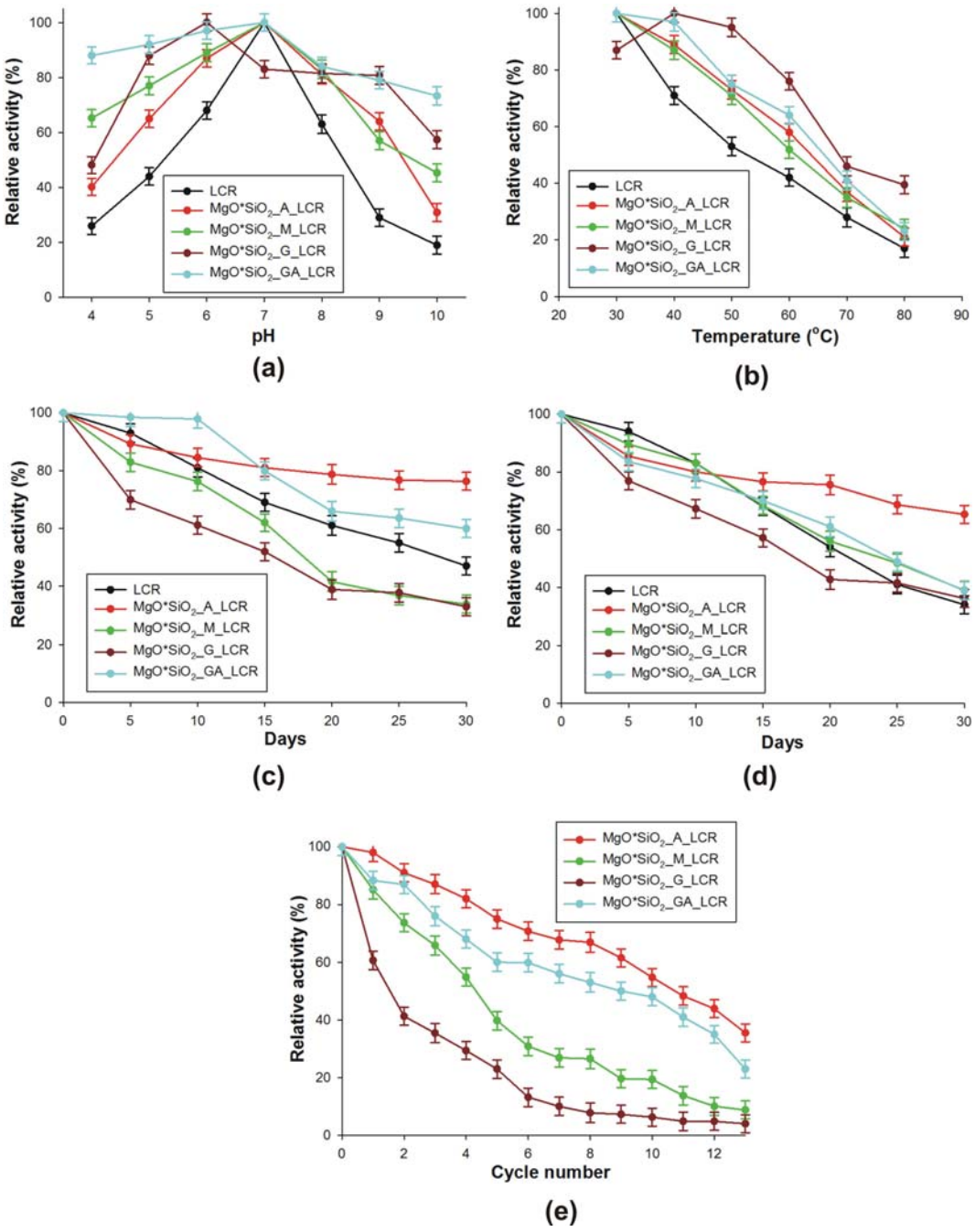

Fig. 9. Effect of pH (a) and temperature (b) on the activity of free and immobilized lipase; storage stability of free and immobilized lipase at 5 °C (c) and 20 °C (d); and reusability of lipase immobilized on modified MgO·SiO_2 (e).

were recorded for the samples MgO·SiO_2_C (20%, 8 mg/g) and MgO·SiO_2_P (11%, 6.5 mg/g). Hong et al. [60] obtained similar results for the immobilization of chymotrypsin and lipase on mesoporous silica (SBA-15; 25 mg/g) and silicates (MSU-F; 30 mg/g). Kuwahara et al. [61] immobilized lipase from *Candida antarctica* on materials with different silica shell structures (OSN), achieving the immobilization of 18.9 mg of enzyme per gram of support.

A determination was next made of the effect of pH, temperature and storage on the catalytic activity of the systems with immobilized lipase, as well as the reusability of these systems. These parameters were determined for selected biocatalytic systems (MgO·SiO_2_A_LCR, MgO·SiO_2_M_LCR, MgO·SiO_2_G_LCR, MgO·SiO_2_GA_LCR). These systems were chosen because they exhibited the highest catalytic activities and contained the greatest quantities of immobilized enzyme (Fig. 8). The results obtained are shown in Fig. 9.

Temperature and pH are important parameters that determine the possible applications of biocatalysts in enzymatic reactions. As can be seen from Fig. 9(a), (b), the pure enzyme has the greatest relative activity at pH=7 and 30 °C. For the other values of both

pH and temperature, the activity declined. In the case of the immobilized systems, however, the relative activity remains high (above 40%) over the whole of the analyzed pH range. The catalytic activity of these systems falls with increasing temperature, but they retain a higher activity than the pure enzyme over the whole analyzed temperature range. The catalytic activity of the system MgO·SiO_2_A_LCR does not fall below 70% anywhere in the analyzed pH and temperature ranges. These data imply the formation of stable bonds between the -NH_2 groups of the modifier and the -NH_2 groups in the structure of the enzyme, which leads to an increase in the rigidity of the enzyme structure and improves its stability in harsh reaction conditions. Similar results were obtained by Khoobi et al. [62] in a study of the immobilization of lipase on functionalized polyethylenimine-grafted mesoporous silica spheres, where again the systems following immobilization retained approximately 40% of their initial activity. Tukel et al. [19] and Ozyilmaz et al. [20] used magnesium silicate (Florisil) as a support for, respectively, catalase and glucose oxidase; in the pH range 4-10 the level of activity retained was 40% and 30% in the respective cases.

The curves in Fig. 9(c) show that lipase immobilized on MgO·SiO_2_A and MgO·SiO_2_GA, after being stored at 5 °C for 30 days, retains a higher activity (above 80% and 60% respectively) than the enzyme in its native form. However, the other two systems (MgO·SiO_2_M and MgO·SiO_2_G) have lower activity than the pure lipase. This may be related to the formation of stronger bonds between the lipase and MgO·SiO_2_A or MgO·SiO_2_GA and to the greater quantity of enzyme immobilized on the support surface. Comparison of these results with data from the literature confirms that the supports proposed in this study can be used successfully in immobilization processes. The systems used by Khoobi et al. [62] (lipase on functionalized polyethylenimine-grafted mesoporous silica spheres) retained approximately 50% of their initial activity after 14 days of storage. Abdallah et al. [23] obtained a biocatalytic system (lipase immobilized on porous spherical silicate material) which retained 40% of its activity after 21 days of storage. The immobilized systems stored at 20 °C for 30 days exhibited similar activity (Fig. 9(d)) to that of pure lipase, except in the case of the lipase deposited on the system MgO·SiO_2_A, which retained approximately 80% of its initial activity.

As shown in Fig. 9(e), the systems MgO·SiO_2_A and MgO·SiO_2_GA retained approximately 50% of their initial activity after ten reaction cycles. The system MgO·SiO_2_G retained 40% of its initial activity for up to five cycles, after which it fell off rapidly. The lowest activity was that of MgO·SiO_2_M. These findings may result from the nature of the interactions between the support and the enzyme and from the quantities of enzyme adsorbed on the surfaces of the various supports. Similar results were reported by Abdlallah et al. [23] (40% of activity retained after seven cycles), Kuwahara et al. [44] (40% of initial activity after 10 cycles), Tukel et al. [19] (30% of initial activity after seven cycles) and Ozyilmaz et al. [20] (50% of initial activity after ten cycles). Additionally, we also checked the protein content in the reaction mixture; however, mainly due to the covalent binding of the enzyme to the support, the amount of the detached enzyme was negligible. Thus, we concluded that decrease in the enzyme activity during reusability tests is related mainly to its deactivation caused by the reaction conditions as well as enzyme inhibition by the substrate and products molecules. Moreover, based on the results previously published in ours and other study [63,64] leakage of the enzyme during its reusability at mild conditions (phosphate buffer at pH 7) is restricted.

A comparison of the effects of the various parameters described above (pH, temperature, storage, repeated reaction cycles and type of functional groups) on the catalytic activity of immobilized systems, as determined in the present work and in previous studies, appears in Table 4.

CONCLUSIONS

The present study reports a proof-of-concept for application of MgO·SiO_2 composite oxide system with various functional groups (-NH, -SH, -CN, -C_6H_5, -COC and -C=O) as a support for lipase immobilization. The applied supports have a very well-developed porous structure, and also contain characteristic groups enabling their successful use in the immobilization of enzymes, as it is also proved by the results presented here. The effectiveness of immobilization has been confirmed by FTIR, NMR and BET analysis. More-

Table 4. Comparison of the stability of immobilized enzymes on different mesoporous silicates

Name of sample	Enzyme	Relative activity in pH=4-10 (%)	Relative activity in temperature range 30-80 °C (%)	Relative activity after 30 days (%)		Relative activity (%), number of cycles (-)	Literature
				5 °C	20 °C		
MgO·SiO_2_A_LCR	Lipase	40	20	80	60	60, 10	This study
MgO·SiO_2_M_LCR	Lipase	40	20	40	40	20, 5	This study
MgO·SiO_2_G_LCR	Lipase	40	40	40	40	30, 8	This study
MgO·SiO_2_GA_LCR	Lipase	70	30	60	40	50, 10	This study
Mesoporous silicate (MPS)	Trypsin	-	-	60	60	40, 6	[12]
Florisil (magnesium silicate)	Catalase	40	20	-	-	30, 7	[19]
Florisil (magnesium silicate)	Glucose oxidase	30	-	40	-	50, 10	[20]
PMS	Lipase	-	-	40	-	40, 7	[23]
Mesoporous silica (SBA-15, MSU-F)	Lipase	-	-	-	80	-	[61]
MCM-41	Lipase	40	-	50	-	-	[62]

over, all of the biocatalytic systems exhibit relatively good activity of more than 40% in the whole of the analyzed ranges of pH (4-10) and temperature (30-70 °C). Results also showed that these systems may be used over ten reaction cycles, retaining a relative activity of around 50-70%. The data obtained show that the systems analyzed in this study may be successfully used as biocatalysts in catalytic reactions, and that the type of functional groups supplied by the surface modifier has a significant effect on the quantity of immobilized enzyme and on the activity and stability of the resulting system. However, relatively easy surface modification, high immobilization efficiency and retention of good catalytic properties by immobilized enzyme caused that the above-mentioned support material might easily be used for the immobilization of other biocatalysts resulting in production of biocatalytic systems for application in many branches of industry.

ACKNOWLEDGEMENTS

This work was supported by Poznan University of Technology Research Grant no. 03/32/DSPB/0806/2018.

REFERENCES

1. P. Zucca and E. Sanjust, *Molecules*, **19**, 14139 (2014).
2. D. M. Liu, J. Chen and Y. P. Shi, *Trends Anal. Chem*., **102**, 332 (2018).
3. D. N. Tran and K. J. Balkus, *ACS Catal*., **1**, 956 (2011).
4. H. H. Weetall, *Methods Enzymol*., **44**, 134 (1976).
5. M. Hartmann and X. Kostrov, *Chem. Soc. Rev*., **42**, 6277 (2013).
6. L. Cao, Carrier-bound immobilized enzymes: principles, application and design, Wiley, New York (2006).
7. Z. Zhou and M. Hartmann, *Top. Catal*., **55**, 1081 (2012).
8. C. Mateo, J. M. Palomo, G. Fernandez-Lorente, J. M. Guisan and R. Fernandez-Lafuente, *Enzyme Microb. Technol*., **40**, 1451 (2007).
9. J. Zdarta, A. S. Meyer, T. Jesionowski and M. Pinelo, *Catalysts*, **8**, 92 (2018).
10. M. Hartmann and X. Kostrov, *Chem. Soc. Rev*., **42**, 6277 (2013).
11. K. Kato, R. Irimescu, T. Saito, Y. Yokogawa and H. Takahashi, *Biosci., Biotechnol., Biochem*., **67**, 203 (2003).
12. D. Goradia, J. Cooney, B. K. Hodnett and E. Magner, *J. Mol. Catal. B-Enzym*., **32**, 231 (2005).
13. J. Forde, A. Vakurov, T. D. Gibson, P. Millner, M. Whelehan, I. W. Marison and C. O'Fagain, *J. Mol. Catal. B-Enzym*., **32**, 231 (2005).
14. T. Jesionowski, J. Zdarta and B. Krajewska, *Adsorption*, **20**, 801 (2014).
15. B. Zhao, X. Liu, Y. Jiang, L. Zhou, Y. He and J. Gao, *Appl. Biochem. Biotechnol*., **173**, 1802 (2014).
16. Y. Wan and D. Y. Zhao, *Chem. Rev*., **107**, 2821 (2007).
17. F. Hoffman, M. Cornelius, J. Morell and M. Froba, *Angew. Chem. Int. Ed. Engl*., **45** 3216 (2006).
18. E. Magner, *Chem. Soc. Rev*., **42**, 6213 (2013).
19. S. S. Tukel and O. Alptekin, *Process Biochem*., **39**, 2149 (2004).
20. G. Ozyilmaz, S. S. Tukel and O. Alptekin, *J. Mol. Catal. B-Enzym*., **35**, 154 (2005).
21. M. Hartmann and D. Jung, *J. Mater. Chem*., **20**, 844 (2010).
22. S. Hudson, J. Cooney and E. Magner, *Angew. Chem. Int. Ed. Eng*., **47**, 8582 (2008).
23. N. H. Abdallah, M. Schlumpberger, D. A. Gaffney, J. P. Hanrahan, J. M. Tobin and E. Magner, *J. Mol. Catal. B-Enzym*., **108**, 82 (2014).
24. W. Liu and L. N. Wei, *J. Mol. Catal*., **30**, 182 (2016).
25. X. Y. Wang, G. Tian, N. Jiang and B. L. Su, *Energy Environ. Sci*., **5**, 5540 (2012).
26. W. Xie and J. Wang, *Energy Fuels*, **28**, 2624 (2014).
27. Z. Chen, L. Liu, X. Wu and R. Yang, *RSC Adv*., **6**, 108583 (2016).
28. W. Xie and X. Zang, *Food Chem*., **257**, 15 (2018).
29. W. Xie and X. Zang, *Food Chem*., **194**, 1283 (2016).
30. Q. Y. Li, P. Y. Wang, Y. L. Zhou, Z. R. Nie and Q. Wei, *J. Sol-Gel Sci. Technol*., **78**, 523 (2016).
31. W. Xie and M. Huang, *Energy Convers. Manage*., **159**, 42 (2018).
32. M. Heidanzadeh, E. Doustkhah, S. Rostamnia, P. F. Rezaei, F. D. Harzevili and B. Zeynizadeh, *Int. J. Biol. Macromol*., **101**, 696 (2017).
33. L. S. Wan, B. B. Ke and Z. K. Xu, *Enzyme Microb. Technol*., **42**, 332 (2008).
34. W. Xie and X. Zang, *Food Chem*., **227**, 397 (2017).
35. Ł. Klapiszewski, J. Zdarta, K. Antecka, K. Synoradzki, K. Siwinska-Stefanska, D. Moszyński and T. Jesionowski, *Appl. Surf. Sci*., **422**, 94 (2018).
36. J. Zdarta, K. Antecka, A. Jędrzak, K. Synoradzki, M. Łuczak and T. Jesionowski, *Colloids Surf., B: Biointer*., **169**, 118 (2018).
37. F. Ciesielczyk, J. Gościańska, J. Zdarta and T. Jesionowski, *Colloids Surf., A: Physicochem. Eng. Aspects*, **545**, 39 (2018).
38. M. W. Ambrogio, C. R. Thomas, Y. L. Zhao, J. L. Zink and J. F. Stodart, *Acc. Chem. Res*., **44**, 903 (2011).
39. Y. T. Zhu, X. Y. Ren, Y. M. Liu, Y. Wei and L. S. Qiang, *Mater. Sci. Eng*., **38**, 278 (2014).
40. Z. Lei, X. Liu, L. Ma, D. Liu, H. Zhong and Z. Wang, *RSC Adv*., **5**, 38665 (2015).
41. F. Ciesielczyk, A. Krysztafkiewicz and T. Jesionowski, *J. Mater. Sci*., **42**, 3831 (2007).
42. T. Jesionowski and A. Krysztafkiewicz, *Appl. Surf. Sci*., **172**, 18 (2001).
43. T. Jesionowski and A. Krysztafkiewicz, *J. Non-Cryst. Solids*, **277**, 45 (2000).
44. F. Ciesielczyk, M. Nowacka, A. Przybylska and T. Jesionowski, *Colloids Surf., A: Physicochem. Eng. Aspects*, **376**, 21 (2011).
45. F. Ciesielczyk, A. Krysztafkiewicz and T. Jesionowski, *Appl. Surf. Sci*., **253**, 8435 (2007).
46. M. M. Bradford, *Anal. Biochem*., **7**, 248 (1976).
47. K. Siwinska-Stefanska, F. Ciesielczyk, M. Nowacka and T. Jesionowski, *J. Nanomater*., **2012**, Article ID 316173, 19 (2012), doi: 10.1155/2012/316173.
48. J. Zdarta, K. Sałek, A. Kołodziejczak-Radzimska, K. Siwińska-Stefańska, K. Szwarc-Rzepka, M. Norman, Ł. Klapiszewski, P. Bartczak, E. Kaczorek and T. Jesionowski, *Open. Chem*., **13**, 138 (2015).
49. F. Ciesielczyk, P. Bartczak, J. Zdarta and T. Jesionowski, *J. Environ. Manage*., **204**, 123 (2017).
50. P. C. Ma, J. K. Kim and B. Z. Tang, *Carbon*, **44**, 3232 (2006).
51. A. Natalello, D. Ami, S. Brocca, M. Lotti and S. M. Doglia, *Biochem. J*., **385**, 511 (2005).
52. T. Raghavendra, A. Basak, L. Manocha, A. Shah and D. Madamwar, *Bioresour. Technol*., **140**, 103 (2013).
53. A. Kołodziejczak-Radzimska, J. Zdarta and T. Jesionowski, *Biotech-*

nol. Progr., **34**, 767 (2018).
54. J. Zdarta, Ł. Klapieszewski, M. Wysokowski, M. Norman, A. Kołodziejczak-Radzimska, D. Moszyński, H. Ehrlich, H. Maciejewski, A. L. Stelling and T. Jesionowski, *Mar. Drugs*, **13**, 2424 (2015).
55. K. Banjanac, M. Mihailovic, N. Prlainovic, M. Corovic, M. Carevic, A. Marinkovic and D. Bezbradic, *J. Chem. Technol. Biotechnol.*, **91**, 2654 (2016).
56. X. Liu, Y. Fang, X. Yang, Y. Li and C. Wang, *Chem. Eng. J.*, **336**, 456 (2018).
57. K. Li, Y. Fan, Y. He, L. Zeng, X. Han and Y. Yan, S*cientific Reports*, **7**, 1 (2017).
58. C. Gunathilake and M. Jaroniec, *J. Mater. Chem.*, **4**, 10914 (2016).
59. H. Takahashi, B. Li, T. Sasaki, C. Miyazaki, T. Kajino and S. Inagaki, *Chem. Mater.*, **12**, 3301 (2000).
60. S. G. Hong, B. C. Kim, H. B. Na, J. Lee, J. Youn, S. W. Chung, C. W. Lee, B. Lee, H. S. Kim, E. Hsiao, S. H. Kim, B. G. Kim, H. G. Park, H. N. Chang, T. Hyeon, J. S. Dordick, J. W. Grate and J. Kim, *Chem. Eng. J.*, **322**, 510 (2017).
61. Y. Kuwahara, T. Yamanishi, T. Kamegawa, K. Mori and H. Yamashita, *ChetCatChem*, **5**, 2527 (2013).
62. M. Khoobi, S. F. Motevalizadeh, Z. Asadgol, H. Forootanfar, A. Shafiee and M. A. Faramarzi, *Biochem. Eng. J.*, **88**, 131 (2014).
63. Ł. Klapiszewski, J. Zdarta and T. Jesionowski, *Colloids Surf., B: Biointer.*, **162**, 90 (2018).
64. A. Straksys, T. Kochane and S. Budriene, *Food Chem.*, **211**, 294 (2016).